TECHNICKÁ UNIVERZITA V LIBERCI

FAKULTA TEXTILNÍ

Vijaykumar Baheti

RENEWABLE NANOSCALE REINFORCEMENT OF BIODEGRADABLE POLYMERS

AUTOREFERÁT DISERTAČNÍ PRÁCE

Název disertační práce:	**RENEWABLE NANOSCALE REINFORCEMENT OF BIODEGRADABLE POLYMERS**
Autor:	**Vijaykumar Baheti**
Obor doktorského studia:	textilní materiálové inženýrství
Forma studia:	prezenční
Školící pracoviště:	KMI
Školitel:	Prof. Ing. Jiri Militky, CSc
Školitel specialista:	

Liberec 2013

1. Objectives

The objectives of the study are

1.1 Extraction and characterization of jute nanofibrils

The main objective of the work is to obtain cellulose based jute nanofibrils (JNF) on large scale quantity from waste jute fibers using environment friendly method of extraction. The wet pulverization of fibers using high energy planetary ball milling process is selected to serve this purpose. During the process of ball milling, fibers tend to defibrillate under the shearing action of frictional force of balls and subsequently refine to nanosegments due to the impact force. The rate of refinement of jute fibers during the process of wet milling is evaluated by characterizing the size of nanofibrils using dynamic light scattering, BET surface area, and field emission scanning electron microscope (FESEM).

1.2 Reinforcement of jute nanofibrils in biopolymers

The obtained wet milled JNF are later incorporated into poly vinyl alcohol (PVA) and poly lactic acid (PLA) biopolymers for preparation nanocomposite films which can be used in the applications of biodegradable food packaging, agriculture mulch covers, etc. The incorporation of JNF is expected to improve the mechanical, thermal and gas barrier properties of semi-crystalline polymeric films. The improvements in mechanical properties are investigated from the morphology and crystallization behavior of composite films using differential scanning calorimetry, tensile tests, dynamic mechanical analysis tests, nanoindentation tests, etc. In order to have the basic understanding of the stiffening, strengthening and toughening properties of JNF in polymeric matrix, the critical evaluation of experimental results with theoretical models is also performed. The popular theories of composites like rule of mixture, Halpin-Tsai, Cox-Krenchel and percolation are employed for validation of obtained results.

2. Overview of current situation

The increased demands of textiles brought the challenges to dispose significant amount of wastes generated during the processing [1,2]. In the context of environment protection and current disposal of the textile wastes, it becomes essential to recover useful products from the wastes for economic reasons. Traditionally, textile wastes are converted to individual fiber stage through cutting, shredding, carding, and other mechanical processes. The fibers are then rearranged into products for applications in garment linings, household items, furniture upholstery, automotive carpeting, automobile sound absorption materials, carpet underlays, building materials for insulation and roofing felt, and low-end blankets [1,2]. However, due to recent increase in competition and reduced profit margins in these industries, it has became important to search for new recycling techniques of waste textiles in order to utilize them for high end applications. One such interesting way is to separate the nanofibrils or nanocrystals from the textile wastes and subsequently incorporate them as fillers into high performance composite materials [3-5].

Cellulose fibers are popularly used in the textile industry due to their high aspect ratio, acceptable density, good tensile strength and modulus [3]. These properties make them attractive class of textile materials traditionally used in manufacture of yarn by spinning process. But, due to certain limitations of the spinning process, shorter fibers (i.e. less than 10 mm) generated during mechanical processing are not suitable to reuse in yarn manufacture and consequently result into the waste [3]. In order to exploit the intrinsic mechanical properties of short cellulose fibers in textile industries, the idea of separating nanofibrils or nanocrystals of cellulose could provide interesting applications in other fields. The previous studies have reported the remarkable properties of cellulose materials at nanoscale dimensions

[4-5]. The extreme improvement in mechanical properties, in the range of 130-160 GPa, of cellulose nanofibrils is attributed to their increased rigidity obtained from parallel arrangement of molecular chains without folding [5]. As a result cellulose nanofibrils have been increasingly used in applications of reinforced biodegradable nanocomposites, foams, aerogels, optically transparent functional materials, and oxygen-barrier layers [7].

The utilization of different types of cellulosic wastes has been studied in the past in order to obtain cellulose nanofibrils at reasonably lower cost. The variety of agricultural wastes like coconut husk fibers [8], cassava bagasse [9], banana rachis [10], mulberry bark [11], soybean pods [12], wheat straw and soy hulls [13] and cornstalks [14], woods are investigated for extraction of cellulose nanofibrils. However, there is no information available in literature on utilization of cellulosic wastes in textile industries in spite of large amount of short fibers are generated during the mechanical processing of yarn manufacture.

Although the cellulose nanostructures have a great potential for reinforcement into biopolymers, the major challenge in order to use them is the extraction. The variety of techniques like acid hydrolysis [15], enzymatic hydrolysis [16], ultrasonication [17], high pressure homogeneization [18], etc have been employed. However, most of these techniques used in the extraction are time consuming, expensive in nature and low in yields [5]. The commonly used strong acid hydrolysis method has a number of important drawbacks such as potential degradation of the cellulose, corrosivity and environmental incompatibility [19]. In order to promote the commercialization of cellulose nanofibrils, the development of more flexible and industrially viable processing technique is needed.

3. Experimental methods

3.1 Materials

Short waste jute fibers were obtained from India. The fibers were measured to have a density of 1.58 g/cm^3, modulus of 20 GPa, tensile strength of 440 MPa and elongation of 2 %. The chemical composition of fibers was reported as cellulose (60 %), hemicelluloses (20 %), lignin (10 %) and others (10 %). Poly lactic acid (PLA) was purchased from NatureWorks LLC, USA through local supplier Resinex, Czech Republic. The PLA had a density of 1.25 g/cm^{3}and the average molecular weight (Mw) of 200,000. The chloroform which was used as solvent, purchased from Thermofisher, Czech Republic.

3.2 Pulverization of jute fibers to nanofibers

3.2.1 Removal of non-cellulosic contents. Chemical pre-treatment of waste jute fibers was carried out before wet pulverization, sequentially with 4 wt % sodium hydroxide (NaOH) at 80°C for 1 hour and with 7 g/l sodium hypochlorite (NaOCl) at room temperature for 2 hours under pH 10-11. Subsequently the fibers were antichlor treated with 0.1 % sodium sulphite at 50°C for 20 min.

3.2.2 Preparation of nanoscale jute fibers. After getting the optimum milling parameters of ball milling process, wet pulverization of waste jute fibers was carried out in distilled water using a high-energy planetary ball mill of Fritsch pulverisette 7. The sintered corundum container of 80 ml capacity and zirconium balls of 3 mm diameter were chosen for 3 hours of wet milling. The ball to material ratio (BMR) was kept at 10:1 and the speed was kept at 850 rpm with reverse rotation of containers. At the end of wet milling, jute particles were separated from water by centrifugation at 4000 rpm and simultaneously transferred in solvent isopropanol to avoid hornification during drying.

Ball milling process is a mechanical process which relies on the energy released at the point of collision between balls as well as on the high grinding energy created by friction of balls on the wall as shown in (Figure 1).

3.2.3 Characterization of nanoscale jute fibers. Particle size distribution of wet milled jute particles was studied after each hour of milling on Malvern zetasizer nano series

based on dynamic light scattering principle of brownian motion of particles. Deionized water was used as dispersion medium and it was ultrasonicated for 5 min with bandelin ultrasonic probe before characterization. Refractive index of 1.52 was used to calculate particle size of wet milled jute. In addition, morphologies of wet milled jute particles were observed on scanning electron microscope (SEM) of TS5130-Tescan at 30 KV accelerated voltage and on field emission scanning electron microscope (FESEM) of Zeiss at 5kV accelerated voltage. The amount of 0.01 g of jute particles was dispersed in 100 ml acetone and then a drop of the dispersed solution was placed on aluminum foil and gold coated after drying. The surface area of the samples was measured from N_2 adsorption–desorption isotherms at 77.35 K using Quantachrome Instruments.

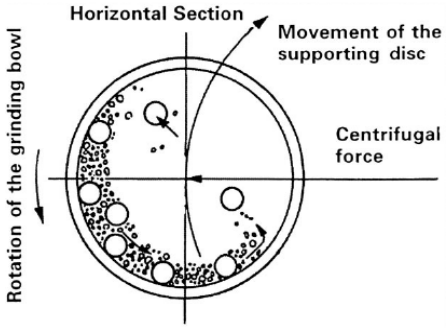

Fig. 1 Principle of working of ball mill [19]

3.3 Preparation of nanocomposite films

PLA/jute nanofibrils composite films with 1, 5 and 10 wt % filler content were prepared by mixing the calculated amount of jute nanofibrils with 5 % PLA in chloroform solution using a magnetic stirrer. The stirring was performed at room temperature for 3 hours. The composite mixture was further ultrasonicated for 10 min on Bandelin Ultrasonic probe mixer with 50-horn power. The final mixtures were then cast on a Teflon sheet. The films were kept at room temperature for 2 days until they were completely dried and then removed from the Teflon sheet. Neat PLA film was also prepared without addition of jute nanofibrils as a reference sample for comparison purpose.

3.4 Testing of nanocomposite films

3.4.1 Differential scanning calorimetry (DSC). The melting and crystallization behavior of the neat and composite films were investigated on DSC 6 Perkin Elmer instrument using pyris software under nitrogen atmosphere with sample weight of 7 mg. The sample was heated from 25°C to 200°C at a rate of 5°C/min. The crystallinity (%) of the PLA was estimated from the enthalpy for PLA content in the nanocomposites, using the ratio between the heat of fusion of the studied material and the heat of fusion of an infinity crystal of same material from Eq.(1)

$$\%\,Crystallinity = \left(\Delta H / w.\Delta H_0\right) \times 100\% \qquad (1)$$

Where ΔH_f is heat of melting of sample, ΔH_0 is heat of melting of 100 % crystalline PLA i.e. 93 j/g [24] and w is mass fraction of PLA in nanocomposite.

3.4.2 Dynamic mechanical analysis (DMA). Dynamic mechanical properties of the nanocomposite films were tested on DMA DX04T RMI instrument, Czech Republic in tensile mode. The measurements were carried out at constant frequency of 1 Hz, strain amplitude of 0.05%, temperature range of 35–100°C, heating rate of 5°C/min and gap distance of 30 mm. The samples were prepared by cutting strips from the films with a width of 10 mm. Four samples were used to characterize each material.

3.4.3 Tensile testing and morphology of fractured surfaces. Tensile testing was carried out using a miniature material tester Rheometric Scientific MiniMat 2000 with a 1000 N load cell at a crosshead speed of 10 mm/min. The samples were prepared by cutting strips from the films with a width of 10 mm. The length between the grips was 100 mm. Total of 10 samples were used to characterize each material. The interaction of JNF and PLA matrix was investigated from fractured surfaces after tensile testing using scanning electron microscope (SEM) TS5130-Tescan SEM at 20 KV accelerated voltage.

4. Results and discussions

4.1 Effect of milling condition on particle size reduction of jute fibers

Under one hour dry milling, jute fibers were pulverised to microparticles with average size of 1480 nm in wider particle size distribution as shown in Figure 2(a) and Figure 3(a). The reason behind multimodal distribution of particles was due to increase in temperature within the mill because of continuous impact of balls. The increased temperature of mill rendered the jute particles to undergo cold welding and deposited a layer on the surface of container and balls as milling progressed. The growth of deposited layer on the milling media changed the impact force of balls on the material with least impact on particles at bottom of layer. In case of wet milling, the increase in temperature was slowed down by deionised water which consequently resulted in narrow particle size distribution with significant reduction in average particle size to 640 nm after one hour of wet milling as shown in Figure 2(b) and Figure 3(b). This can be attributed to uniformity in impact action of balls on every individual particle in wet condition.

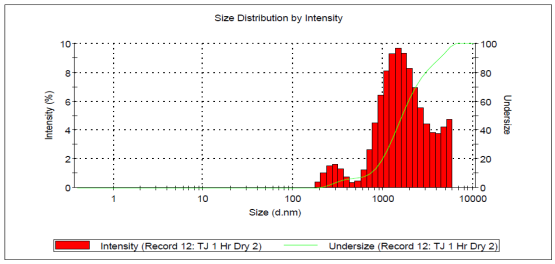

(a) One hour dry milling

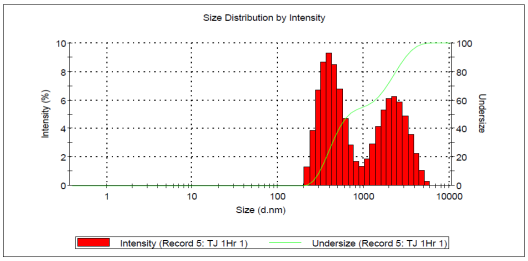

(b) One hour wet milling

Fig. 2 Particle size distribution of jute particles

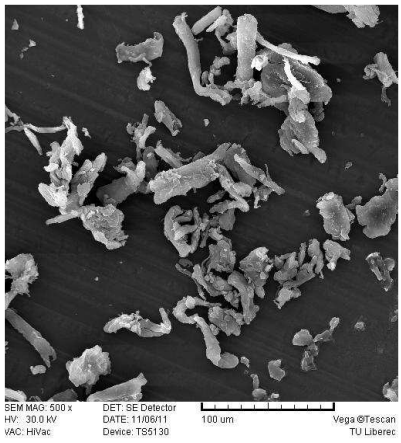

a) One hour dry milling

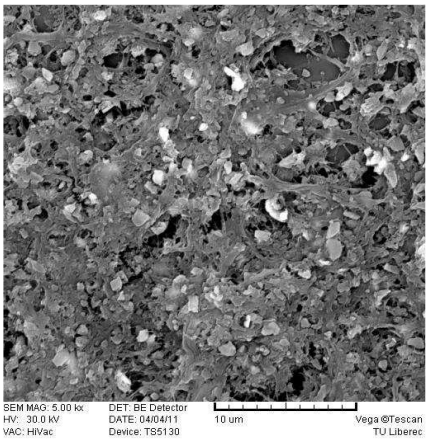

b) One hour wet milling

Fig. 3 SEM image of jute particles

4.2 Effect of wet milling time on particle size reduction of jute fibers

To further refine the jute particles to smaller size, wet milling was performed for extended duration. The average particle size reached to 443 nm after 3 hours of wet milling and the particle size distribution changed slowly from multimodal nature to unimodal nature as shown in Figure 4. This showed the consistency and homogeneity in milling action on every individual particle as milling continued for longer time. However the rate of refinement became slower while grinding the smaller particles in addition to the severe damage of milling balls due to direct collision. This could have introduced some inorganic contaminations from mill to the material, so further pulverization was stopped and jute particles in 500 nm range were used as nano/micro fillers.

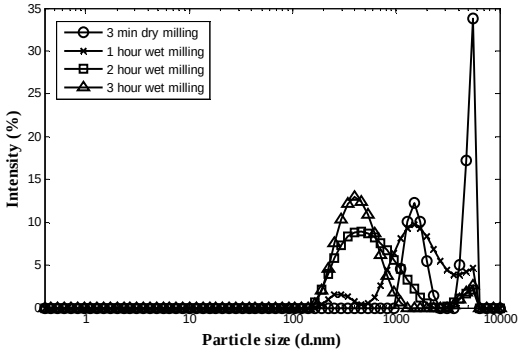

Fig. 4 Effect of extended wet milling time on particle size reduction

The shape and size of jute fibers after three hours of wet milling was precisely investigated with the help of FESEM image (Figure 5a) due to its better resolution at nanoscale. The shape of jute particles was seen in the form of nanofibrils with certain aspect ratio. The few jute particles without aspect ratio were considered as agglomerates of hundreds of individual jute nanofibrils. In order to measure the diameter of nanofibrils, NIS Elements BR software was employed and total of 25 observations were made. The probability density function of diameter distribution of 25 readings is shown in Figure 5b. In this way, the mean diameter and standard deviation was calculated as 46.52 nm and 13.58 nm respectively.

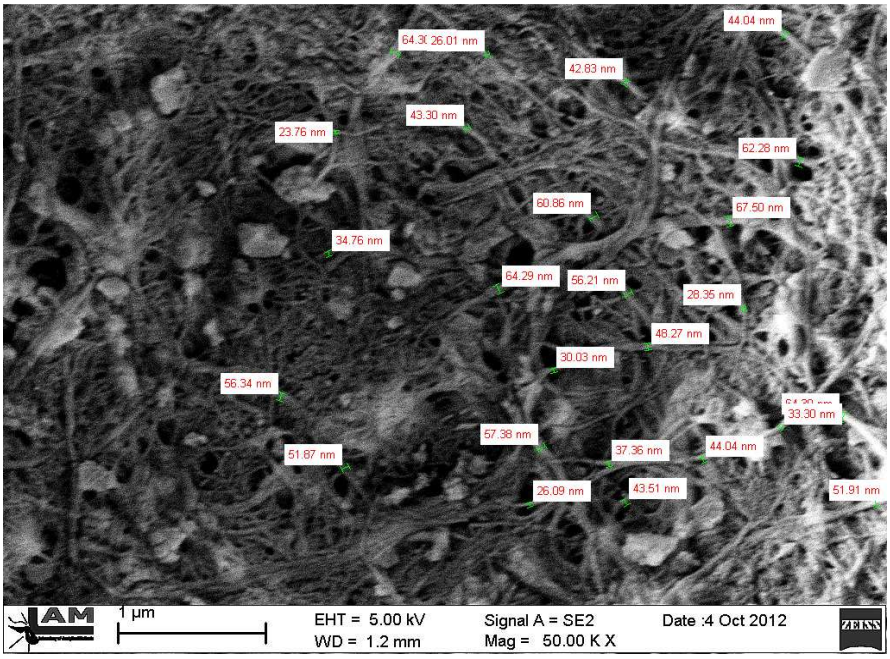

Fig. 5(a) SEM image of jute nanofibrils

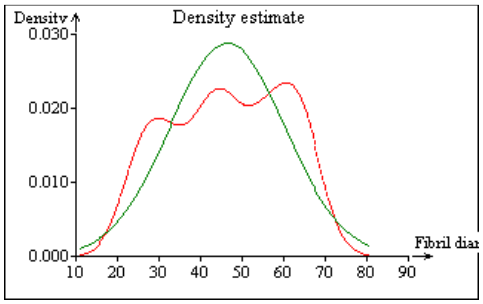

Fig. 5(b) Probability density function of diameter distribution of jute nanofibrils

4.3 Comparison of size measured on different techniques

The size of nanofibrils obtained after dry and wet pulverization of jute fibers is compared on the basis of different techniques of measurements as given in Table 1. The techniques based on DLS and BET measurements found to overestimate the size of nanofibrils with regard to actual size. The size obtained after image analysis found much lesser as compared to DLS and BET measurements. The significant difference in size is attributed to the principles of working of different techniques which are based on certain assumptions. The DLS and BET techniques assume the shape of particles as spherical while calculating the particle size, whereas image analysis measurements are based on actual projected image of particles.

Table 1. Comparison of jute nanofibril size from different techniques

Sample Name	DLS Technique (Spherical shape)	BET Technique (Spherical shape)	Image analysis (Actual shape)
One hour dry milling	1480 nm	1120 nm	480 nm
One hour wet milling	619 nm	430 nm	85 nm
Three hour wet milling	493 nm	190 nm	46 nm

4.4 DSC of PLA/JNF composite films

Table 2 shows that T_g value of PLA increased with the increased loading of JNF. The maximum improvement was observed in case of 10 wt % of JNF where T_g was increased from 42^{o}C to 49^{o}C as compared to the neat PLA film. The T_g is a complex phenomenon which depends on intermolecular interactions, steric effects, chain flexibility, molecular weight, branching and the cross-linking density [20]. The corresponding increase in value of T_g by 1.15 %, 8.64 % and 15.70 % over neat PLA film can be attributed to the reduced PLA chain flexibility after addition of 1 wt %, 5 wt % and 10 wt % JNF respectively.

With the addition of JNF, the cold crystallization peak found to become broader and shifted to lower temperatures as compared to the cold crystallization of neat PLA (Figure 6). The lower T_{cc} observed in the heating run can be an indication of faster crystallization induced by JNF which act as nucleating agents for PLA [21]. This increase of crystallinity confirms the previous observations related to the role of cellulose nanofibrils as nucleating agents [22-23].

It is clear from Table 2 and Figure 6 that T_m of PLA improved at lower loading of JNF and then remained constant. The increase in T_m from 147.49^{o}C to 153.15^{o}C after addition of 1 wt % JNF can be attributed to the increased crystallinity of PLA due to nucleating ability of JNF [22]. However, constant value of T_m at 153^{o}C with increase in JNF content is attributed to the increased entanglements of JNF, which restricted the capability of the matrix chains to grow bigger crystalline domains [24]. A more careful observation of the thermograms of the nanocomposites reveals the presence of small endotherms just before the main melting peaks. The similar observation of bimodal melting peak of PLA is reported in previous work [22]. The melting peak at higher temperature (T_{m2}) was attributed to a more perfect crystalline

structure of PLA and the shoulder peak at lower temperature (T_{m1}) to a less perfect crystalline structure. This indicated that PLA develops more heterogeneous crystalline morphology after addition of JNF.

The crystallinity of PLA composite films increased by 20.00 %, 44.06 % and 62.15 % compared to neat PLA films, after addition of 1 wt %, 5 wt % and 10 wt % JNF respectively. The maximum increase in crystallinity was observed in case of 10 wt % JNF-PLA composite film. This behavior agrees with a previous work on PHBV [25]. The increased crystallinity of PLA in composites with increased JNF content is attributed to the increased area of nucleating nanofibrils responsible for transcrystallization of PLA [26].

Table 2. Behavior of neat and JNF/PLA composite films on application of heat

Sample	T_g (^oC)	T_{cc}(^oC)	T_m(^oC)	ΔH (J/g)	Crystallinity%
Neat PLA	42.35±0.3	98.85±1.1	147.49±0.1	17.33±2.8	18.63
1% JNF+PLA	42.84±0.5	97.90±1.2	153.15±0.1	20.52±3.0	22.28
5% JNF+PLA	46.01±0.6	97.70±1.4	153.14±0.2	24.74±3.3	26.84
10% JNF+PLA	49.00±1.2	96.43±1.5	153.97±0.5	26.38±3.6	30.21

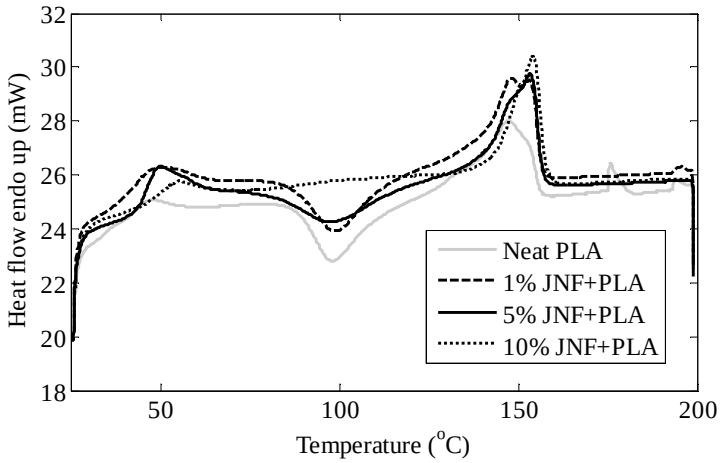

Fig. 6 DSC of neat and JNF/PLA composite films

4.5 Dynamic mechanical analysis (DMA) of PLA/JNF composites

The load bearing capacity of neat PLA and PLA composite films was studied from the storage modulus results shown in the Figure 7(a) and Table 3. The storage modulus of the PLA composite films improved over the entire temperature span compared to neat PLA. The maximum improvement was observed in case of 5 wt % nanocomposite where storage modulus was increased from 3.0 GPa to 9.0 GPa at 35^{o}C. This increase in storage modulus value is attributed to the higher stiffness of JNF during the transfer of stress from the matrix to nanofibrils [27]. However with further increase in loadings of JNF to 10 wt %, storage modulus reduced to 5.0 GPa because of poor dispersion and agglomerations of nanofibrils [22]. With the increase in temperature, the storage modulus of neat PLA dropped at faster rate than PLA composites. The significant drop in storage modulus of neat PLA at 60^{o}C is due to the softening of matrix and easier movement of PLA chains. The relatively smaller drop in case of composites is attributed to the presence of JNF which restricted the motion of PLA chains [22]. At 60^{o}C, PLA composite films of 1 wt %, 5 wt % and 10 wt % JNF showed 8.33 %, 475.00 %, and 364.58 % respective increase in storage modulus compared to neat PLA films. The higher storage modulus values of PLA composite films compared to neat PLA above 60^{o}C are attributed to the nucleating behavior of JNF which improved crystallinity of PLA through transcrystallization. The ratio of loss modulus to storage modulus is defined as mechanical loss factor or tan delta. Figure 7(b) showed that the tan delta peak of PLA (T_α)

was positively shifted with increased content of JNF in composites. The shift of 5°C, 12°C and 15°C was observed in case of 1 wt %, 5 wt % and 10 wt % nanocomposites respectively. The positive increments in shift of tan delta are attributed to the increased surface area of interaction between the matrix and nanofibrils which restricted the segmental mobility of the matrix chains around them [28].

Table 3. Storage modulus of neat and JNF/PLA composite films at different temperature

Sample name	T_α	E' (T_α) (GPa)	E' (35 °C) (GPa)	E' (60 °C) (GPa)
Neat PLA	40±1	2.42±0.15	3.09±0.20	0.48±0.02
1% JNF+PLA	45±1	4.53±0.35	5.85±0.46	0.52±0.04
5% JNF+PLA	50±2	6.58±0.50	9.14±0.80	2.76±0.21
10% JNF+PLA	60±3	2.23±0.24	5.31±0.55	2.23±0.26

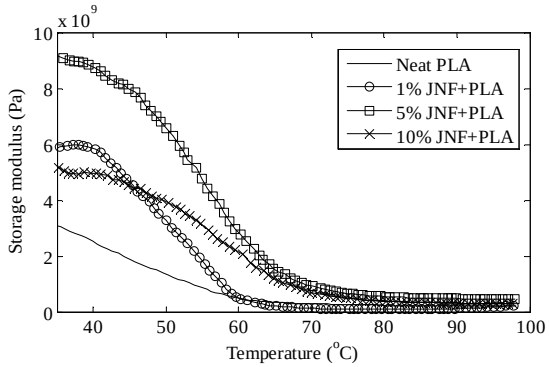

Fig. 7(a) Storage modulus of neat and JNF/PLA composite films

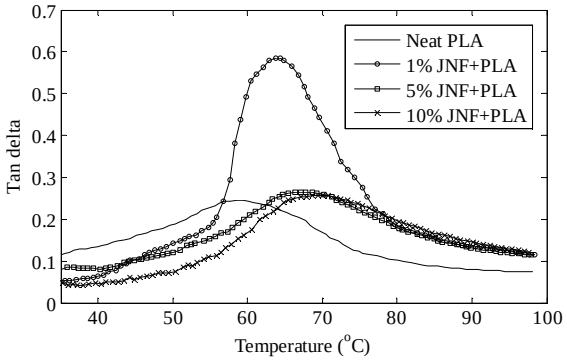

Fig. 7(b) Damping factor of neat and JNF/PLA composite films

4.6 Tensile testing of PLA/JNF composites

Figure 8 shows typical stress–strain curves of neat PLA and its composite films with different nanofibril contents and Table 4 shows the average values and standard deviations of the mechanical properties. The large standard deviations of mechanical properties indicated non-homogeneous dispersion of nanofibrils at higher loading. The stress-strain curve clearly shows that both tensile strength and initial modulus are higher for 1 wt % and 5 wt % JNF/ PLA composite films compared to neat PLA and elongation to break are lower in all composite films compared to neat PLA.

The composite films with 1 wt % and 5 wt % JNF contents showed 121.70 % and 170.59 % respective increase in tensile strength compared to neat PLA. The increase in strength is an indication of better stress transfer across the interphase, which means that there is practically good interfacial bonding between JNF and the polymer matrix. However, the trend of increase in tensile strength with increase in JNF content failed at 10 wt % loading of JNF. The significant reduction of 17.62 % in tensile strength with addition of 10 wt % JNF can be attributed to increased agglomerations and reduced surface area of interaction between JNF and PLA matrix [22].

The reduction in elongation to break over neat PLA film was observed in range of 60.95 %, 65.28 % and 65.08 % after addition of 1 wt %, 5 wt % and 10 wt % JNF respectively. As previously discussed in DSC analysis, addition of JNF increased the crystallinity of semicrystalline PLA matrix which consequently resulted in embrittlement of PLA. The lowering of elongation to break in composite films can be attributed to the increase in this brittleness of PLA [29]. In addition, the tendency of stress concentrations due to stiff nature of JNF also explains the lowering of elongation to break of composite PLA films [22].

The initial modulus of PLA composite films increased by 39.42 %, 217. 30 % and 5.76 % as compared with neat PLA films after addition of 1 wt %, 5 wt % and 10 wt % JNF respectively. The maximum increase in initial modulus from 1.04 GPa to 3.30 GPa was observed in case of 5 wt % JNF reinforced PLA films. The increased interaction area between nanofibrils and matrix along with higher crystallinity of PLA in composites attributed to this increase in modulus of the composites [24]. The increase in modulus could also be explained due to formation of rigid network of JNF by hydrogen bonding between adjacent nanofibrils. This percolation effect due to entanglements of cellulose nanofibrils have been studied previously [24]. The significant fall in modulus value at 10 wt % JNF loading explained the possibility of agglomerations and entanglements of JNF at higher loading. The agglomerations reduced the area of interaction between nanofibrils and polymer matrix whereas entanglements reduced the nucleating area of nanofibrils responsible for transcrytallization phenomena [30-31].

Table 4. Tensile properties of neat and JNF/PLA composite films

Sample name	Initial modulus (GPa)	Tensile strength (MPa)	Elongation (%)
Neat PLA	1.04±0.03	25.98±0.13	4.84±0.72
1% JNF+PLA	1.45±0.03	57.60±0.40	1.89±0.34
5% JNF+PLA	3.30±0.05	70.30±0.63	1.68±0.33
10% JNF+PLA	1.10±0.08	21.40±0.32	1.69±0.42

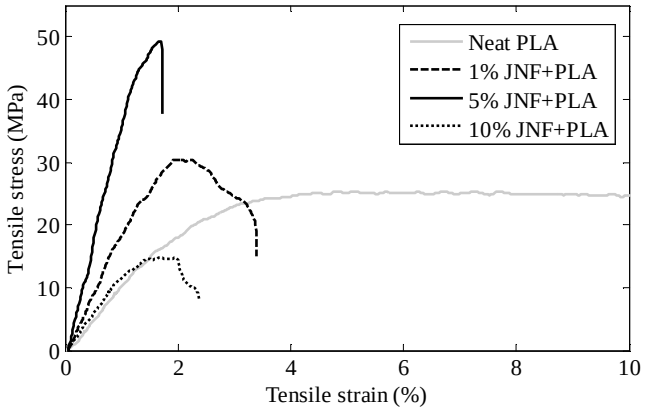

Fig. 8 Stress-strain curve of neat and JNF/PLA composite film

In order to understand the interaction between PLA and JNF, the morphology of fractured surface profiles of neat PLA and nanocomposite PLA films were studied under the SEM as shown in Figure 9. The improvement in mechanical properties depends on absence of voids, intact position of fillers, interfacial bonding between fillers and matrix, and absence of agglomerations of fillers [32]. In the present study, although some agglomerations could be observed in all nanocomposite films, most of the JNF were still kept intact within the PLA matrix for 1 wt % and 5 wt % loading (Figure 9a). This indicated that the extent of interaction between JNF and PLA is better at low JNF loading due to less available surface area of JNF for uniform wetting with PLA. As JNF loading was increased to 10 wt %, the position of JNF in PLA was displaced leading to formation of gap between JNF surface and PLA matrix (Figure 9b). This is a clear indication of poor interfacial adhesion between JNF and PLA at higher loading of JNF [33]. Thus, the 10 wt % JNF/PLA nanocomposite showed significant deterioration in mechanical properties as compared to neat PLA and other composite films.

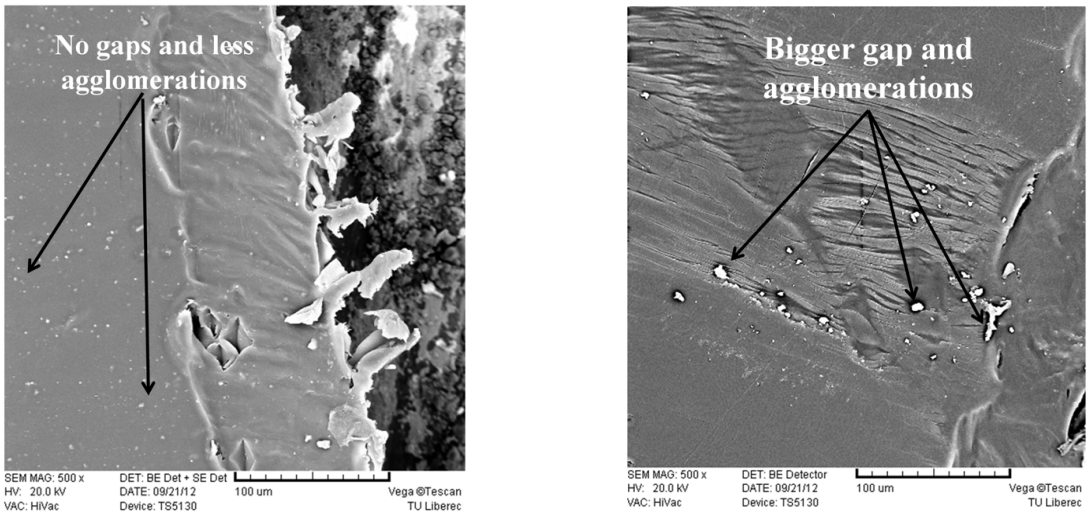

(a) 5% JNF+PLA composite film (b) 10% JNF+PLA composite film

Fig. 9 Fractured surfaces

4.7 Comparison of experimental results with mechanical models

In order to understand the reinforcement potentials of JNF in PLA matrix, the experimental results of Initial modulus were compared with predicted elastic modulus of mechanical models. The improvements in mechanical properties based on filler-matrix interaction are predicted from rule of mixture theory, Halpin-Tsai theory and Cox-Krenchel theory. Whereas, percolation theory is used to predict the properties based on filler-filler interaction due to hydrophilic nature of JNF. The following values were used for theoretical calculations: Modulus of PLA (E_m) = 1.04 GPa, Modulus of JNF (E_r) = 167.5 GPa [34], Density of JNF (ρ_r) =1.58 g/cm^3, and Density of PLA (ρ_m) = 1.25 g/cm^3. The diameter of JNF was taken as 50 nm from the measurements in Figure 2 whereas length of JNF was approximately considered around 5 µm.

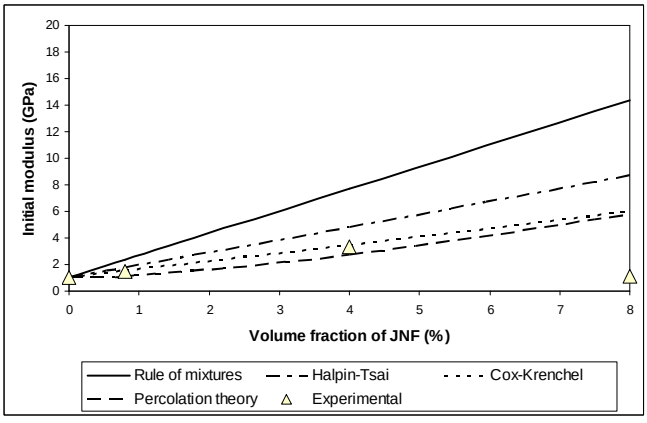

Fig. 10 Comparison of experimental results with mechanical models

The comparison of experimental results of Initial modulus revealed good agreement with predicted elastic modulus of theoretical models up to 5 wt % loading of JNF. It is clear from Figure 10 that experimental results are situated below the predictions of rule of mixture, Halpin-Tsai and Cox-Krenchel theories and are situated above the predictions of percolation theory. This indicated significant scope in improvement of fibril-matrix interaction in

composite films compared to fibril-fibril interaction. The close agreement of experimental Initial modulus with predicted value of Cox-Krenchel theory than Halpin-Tsai theory also suggested random orientation of JNF in PLA composite films. The significant deviation of experimental results from all theories above 5 wt % of JNF content can be attributed to the agglomeration and entanglements of nanofibrils.

5. Author publications on the topic

5.1 International Journals

1. Vijay Baheti, Jiri Militky, Miroslava Marsalkova: Mechanical properties of poly lactic acid composite films reinforced with wet milled jute nanofibers, *Polymer Composites* DOI: 10.1002/pc.22622 (In press).
2. Vijay Baheti, Jiri Militky: Reinforcement of wet milled jute nano/micro particles in PVA films, *Fibers and Polymers*, Vol 14 (2013), pp. 133-137. (ISSN 1229-9197)
3. Vijay Baheti, Rehan Abbasi, Jiri Militky, Jaroslav Dobias: Barrier properties of Poly lactic acid (PLA) packaging films reinforced with ball milled jute micro/nano particles, *Vlakna a Textil*, Vol 19 (2012), pp. 10-16. (ISSN 1335-0617)
4. Vijay Baheti, Miroslava Marsalkova, Rehan Abbasi, Jiri Militky: Comparison of wet milling action for fibrous and solid materials, *Vlakna a Textil*, Vol 19 (2012), pp. 3-7. (ISSN 1335-0617)
5. V.K.Baheti, R. Abbasi, J.Militky: Ball milling of jute fibre waste to prepare nanocellulose, *World journal of engineering*, Vol 9 (2012), pp. 45-50. ISSN (1708-5284).
6. V.K.Baheti, Miroslava Marsalkova, Jiri Militky: Preparation of nanocellulosic powder from jute fibres by ball milling process, *World journal of engineering*, Special edition of ICCE 19 Shanghai, (ISSN 1708-5284).
7. Vijay Baheti, Rehan Abbasi, Jiri Militky: Optimisation of Ball Milling Parameters for Refinement of waste Jute Fibers to Nano/Micro Scale in Dry Conditions, *Journal of Textile Engineering* (In press).
8. Vijay Baheti, Jiri Militky, Rajesh Mishra, B.K. Behera: Influence of noncellulosic contents on nano scale refinement of waste jute fibers for reinforcement in polylactic acid films, *Fibers and Polymers* (Under Review).
9. Vijay Baheti, Vinod VTP, Jiri Militky, Miroslav Cernik, Rajesh Mishra: Removal of mercury from aqueous environment bu jute nanofiber, *Journal of Fiber Bioengineering and Informatics*, Vol 6 (2013), pp 175-184. (ISSN 1940-8676)
10. Vijay Baheti, Jiri Militky, Ul Hassan Z. S.: Polylactic acid composites reinforced with wet milled jute nnaofibers, *Conference Papers in Materials Science* (Under Review).
11. Vijay Baheti, Jiri Militky: Mechanical properties of biodegradable composite films reinforced with jute nanostructures, *World Journal of Engineering* (Submitted).
12. Vijay Baheti, Jiri Militky: Nanoindentation measurements of PLA composite films reinforced with different size jute fibers (Under Preparation).

5.2 International Conference

1. Vijay Baheti, Jiri Militky, Miroslava Marsalkova: Effect of jute fiber size on elastic modulus of poly lactic acid composite films: Investigation from Nanoindentation measurements, Texsci, September 2013, Liberec, Czech Republic.
2. Vijay Baheti, Jiri Militky, Miroslava Marsalkova: Influence of jute nanofibers on softening temperature of poly lactic acid composite films, Texsci, September 2013, Liberec, Czech Republic.

3. Vijay Baheti, Jiri Militky, Rajesh Mishra: Polylactic acid (PLA) films reinforced with wet milled jute nanofibers, ICNF 1, June 2013, Guimaraes, Portugal (ISBN 978-989-20-3872-8).
4. Vijay Baheti, Jiri Militky: Mechanical properties of wet milled jute nanofibers for reinforcement in poly lactic acid films, ICCE 21, July 2013, Tenerife, Spain
5. Vijay baheti, Miroslava Marsalkova, Jiri Militky: Gas barrier properties of PLA films reinforced with wet milled jute nano particles, STRUTEX 19, December 2012, Liberec, Czech Republic. (ISBN 978-80-7372-913-4).
6. Vijay baheti, Miroslava Marsalkova, Jiri Militky: Preparation of nanocellulosic templates for hybrid metal oxide by optimum milling parameters, STRUTEX 19, December 2012, Liberec, Czech Republic. (ISBN 978-80-7372-913-4)
7. Vinod VTP, Vijay Baheti, Jiri Militky, Miroslav Cernik: Jute nanofibre as a natural biosorbent for efficient remediation of Hg2+ ion from aqueous environment, STRUTEX 19, December 2012, Liberec, Czech Republic. (ISBN 978-80-7372-913-4).
8. Vijay Baheti, M. Marsalokova, R. Abbasi, Jiri Militky: Optimisation of milling parameters to prepare nanocellulosic templates for hybrid metal oxides, *Svetlanka workshop 2012*, Liberec, Czech Republic.
9. Vijay Baheti, Rehan Abbasi, Jiri Militky: Influence of ball milling conditions on particle size distribution of fly ash, *NanoOstrava 2*, 27-29 April 2011, Ostrava, Czech Republic (ISBN 978-80-7329-264-5).
10. Vijay Baheti, Jiri Bobek, Jiri Militky: Injection moulded PLA composites reinforced with banana fibre particles obtained after ball milling, 5th International Technical Textile Congress, 7-9 November 2012, Izmir, Turkey (ISBN 978-975-441-377-9).
11. Vijay Baheti, Rehan Abbasi, Jiri Militky: Use of techniques to prepare different forms of nanocellulose from jute fibres, 12th *AUTEX World Textile Conference*, 13-15 June 2012, Zadar, Croatia, (ISBN 978-953710548-8).
12. Vijay Baheti, Rehan Abbasi, Jiri Militky: Optimisation of Ball Milling Parameters for Refinement of Jute Fibres to Nano/Micro Scale in Dry Conditions, *Textile Research Symposium*, 12-14 September 2012, Guimaraes, Portugal.(ISBN 978-972-8063-66-5).
13. Vijay Baheti, Rehan Abbasi, Jiri Militky: Use of techniques to prepare different forms of nanocellulose from jute fibres, *Indutech*, 3-4 August September 2012, Coimbatore, India.
14. Vijay Baheti, Miroslava Marsalkova,Jiri Militky: Preparation of Nanocellulosic Powder from Jute Fibres by Ball Milling Process, *ICCE 19*, 24-30 July 2011, Shanghai, China.
15. Vijay Baheti, Miroslava Marsalkova, Jiri Militky: Preparation of Nanocellulose from Jute Fibres and its Applications as Fillers in Naocomposite Packaging Films, *International Conference, North Indian Section of Textile Institute*,9-10 September 2011,New Delhi India.
16. Vijay Baheti, Rehan Abbasi, Miroslava Marsalkova, Jiri Militky: Comparison of techniques to prepare Nano crystalline cellulose from jute fibres, *STRUTEX 18*, 7-8 December 2011,Liberec, Czech Republic (ISBN 978-80-7372-786-4).
17. Vijay Baheti, Vinod VTP, Jiri Militky, Miroslav Cernik: Use of Jute nanofiber for removal of mercury from aqueous environment, *TBIS* , September 2013, Xian, China (Submitted).
18. Vijay Baheti, Jiri Militky, Rajesh Mishra: Wet milling of waste textile fibers and their reinforcement in biodegradable nanocomposite films, *Textile Research Symposium 2013*, Mount Fuji, Japan (Submitted).

6. References

1. W. Wang, Recycling in textiles, (2006) *Woodhead publishing* UK.
2. R. Horrocks, Recycling textile and plastic waste, (1996) *Woodhead publishing*, UK.
3. C.W.M. Yuen, Y. F. Cheng, Y. Li, and J. Y. Hu, *Journal of Textile Institute*, **100**,165 (2009).
4. H. P. S. Khalil, A. H. Bhat, and A. F. Yusra, *Carbohydrate Polymers*, **87**, 963 (2012).
5. D. Klemm, D. Schumann, F. Kramer, N. Hebler, M. Hornung, H. Schmauder, and S. Marsch, *Advances in Polymer Science,* **205**, 49 (2006).
6. J. Mussig, and C. Stevens, Industrial Applications of Natural Fibers: Structure, Properties and Technical Applications, (2010) *Wiley*.
7. A. Dufresne, M. B. Kellerhals, and B. Witholt, *Macromolecules*, **32**, 7396 (1999).
8. M. F. Rosa, E. S. Medeiros, J. A. Malmonge, K. S. Gregorski, D. F. Wood, L. H. C. Mattoso, G. Glenn, W. J. Orts and S. H. Imam, *Carbohydrate Polymers*, 81, 83 (2010).
9. D. Pasquini, E. D. M. Teixeira, A. A. D. S. Curvelo, M. N. Belgacem and A. Dufresne, *Industrial Crops and Products*, 32, 486 (2010).
10. R. Zuluaga, J. L. Putaux, J. Cruz, J. Velez, I. Mondragon and P. Ganan, *Carbohydrate Polymers*, 76, 51 (2009).
11. R. Li, J. Fei, Y. Cai, Y. Li, J. Feng and J. Yao, *Carbohydrate Polymers*, 76, 94 (2009).
12. B. Wang and M. Sain, *Composite Science and Technology*, 67, 2521 (2007).
13. A. Alemdar and M. Sain, *Bioresource Technology*, 99, 1664 (2008).
14. N. Reddy and Y. Yang, *Polymer*, 46, 5494 (2005).
15. D. Y. Liu, X. W. Yuan, D. Bhattacharyya, and A. J. Easteal, *Express Polymer Letters*, **4**, 26 (2010).
16. P. Satyamurthy, P. Jain, R. Balasubramanya, and N. Vigneshwaran, *Carbohydrate Polymers*, **83**,122 (2011).
17. W. Li, J. Yue, and S. Liu, *Ultrasonics Sonochemistry*, **19**, 479 (2012).
18. J. Leitner, B. Hinterstoisser, M. Wastyn, J. Keches, and W. Gindl, *Cellulose*, **14**, 419 (2007).
19. S. Thomas, and L. A. Pothan, Natural fiber reinforced polymer composites, (2008) *Old City Publishing USA*.
20. E.W. Fisher, H.J. Sterzel, and G. Wegner, *Colloid and Polymer Science*, **251**, 980 (1973).
21. P. Krishnamachari, J. Zhang, J. Lou, J. Yan, and L. Uitenham, *International Journal of Polymer Analysis and Characterization*, **14**, 336 (2009).
22. K. S. Kang, S. I. Lee, T. J. Lee, R. Narayan, and B. Y. Shin, *Korean Journal of Chemical Engineering*, **25**, 599 (2008).
23. B. Suksut, and C. Deeprasertkul, *Journal of Polymers and the Environment*, **19**, 288 (2011).
24. R. Tokoro, D. M. Vu, K. Okubo, T. Tanaka, T. Fujii, and T. Fujiura, *Journal of Materials Science*, **43**,775 (2008).
25. M. Roohani, Y. Habibi, N. M. Belgacem, G. Ebrahim, A. N. Karimi, and A. Dufresne, *European Polymer Journal*, **44**, 2489 (2008).
26. L. Jiang, E. Morelius, J. Zhang, and M. Wolcott, *Journal of Composite Materials*, **42**, 24 (2008).
27. G. Zhang, and D. J. Yan, *Applied Polymer Science*, **88**, 2181 (2003).
28. M. Smita, K. V. Sushil, and K. N. Sanjay, *Composite Science and Technology*, **66**,538 (2006).
29. L. Averous, C. Fringant, and L. Moro, *Polymer*, **42**, 6565 (2001).

30. S. D. Park, M. Todo, and K. Arakawa, *Journal of Material Science*, **39**, 1113 (2004).
31. A. P. Mathew, K. Oksman, and M. Sain, *Journal of Applied Polymer Science*, **97**, 2014 (2005).
32. D. Garlotta, W. Doane, R. Shogren, J. Lawton, and J. L. Willett, *Journal of Applied Polymer Science*, **88**, 1775 (2003).
33. G. H. Yew, A. M. Mohd Yusof, Z. A. Mohd Ishak, and U. S. Ishiaku, *Polymer Degradation and Stability*, **90**, 488 (2005).
34. K. Tsahiro, and M. Kobayaski, *Polymer*, **32**, 1516 (1991).

7. Summary

The goal of present study was to utilize the waste jute fibers in textile industry as a source of cellulose nanofibrils for reinforcement of biodegradable packaging films. The jute nanofibrils were obtained by wet pulverization using high energy planetary ball milling process instead of strong acid hydrolysis due to its simple, economical and environment friendly approach. The extended wet milling for the duration of three hours resulted into unimodal distribution of jute nanofibrils with diameter below 50 nm. In the subsequent step, obtained jute nanofibrils were incorporated at 1 wt %, 5 wt % and 10 wt % loading in PLA matrix and their reinforcement was evaluated based on improvements in mechanical properties. The results showed that improvements in mechanical properties are dependent on interaction between nanofibrils -matrix as well as on crystallinity of PLA in nanocomposites. Due to the possibility of agglomerations and entanglements of nanofibrils at different loading, the surface area of interaction and area of nucleating nanofibrils changed in the composites. This resulted in a large difference in the mechanical properties between all samples. The 5 wt % nanocomposite films showed maximum improvements in mechanical properties, while 10 wt % nanocomposite films revealed deterioration in properties. The improvements in storage modulus of PLA nanocomposite films over neat PLA were more evident at 60^{o}C than 35^{o}C. The storage modulus of 5 wt % nanocomposite films found to improve by only 195.79 % at 35^{o}C, whereas huge improvements in storage modulus by 475.00 % observed at 60^{o}C. The restricted mobility of PLA chains by presence of stiff JNF is attributed to the improvements in load bearing capacity of PLA at higher temperature. The initial modulus and tensile strength were increased by 217. 30 % and 170.59 % respectively in case of 5 wt % nanocomposite compared to neat PLA film. However, elongation to break was found to reduce in all composite films compared to neat PLA film due to increased brittleness, which was induced by increased crystallinity of PLA in composites. The composite films at higher JNF content of 10 wt % revealed deterioration in mechanical properties due to nonhomogeneous stress transfer from matrix to nanofibrils caused by poor dispersion and agglomerations of nanofibrils. However, 15.70 % improvements in T_g and 62.15 % improvements in crystallinity are reported at 10 wt % JNF loading in PLA. This suggested that the deterioration in mechanical properties could be prevented by allowing uniform dispersion and less agglomerations of JNF in nanocomposites. Finally, the experimental results of Initial modulus revealed good agreement with predicted elastic modulus of theoretical models up to 5 wt % loading of JNF. The closeness of experimental results with Cox-krenchel theory suggested random orientation of nanofibrils in the composites. In this way, it is possible to say that in order for nanofibrils to reach their full reinforcing potentials, more attention will have to be given into the dispersion and alignment of nanofibrils within PLA matrix.

VydalaTextilní fakulta, Technické univerzity v Liberci jako interní publikaci pod pořadovým číslem DFT/4/2013 v počtu 20 výtisků